Reliability assessment of train screws subjected to fatigue, corrosion and human errors

Alaa Chateauneuf[a], Francis Cocheteux[b], Franck Deffarges[c] et Florence Sourget[d]

[a] LGC, Université Blaise Pascal, Campus des Cézeaux, BP 206, 63174 Aubière cedex, France
[b] SNCF-Agence d'Essai Ferroviaire, 21 av. Président Allende, 94407 Vitry-sur-Seine, France
[c] SNCF-Centre d'Ingénierie du Matériel 1, Allée des Gémeaux, 72100 Le Mans, France
[d] SNCF-Direction de l'Innovation et de la Recherche, 45 Rue de Londres, 75379 Paris cedex 08, France

Abstract The reliability of railway equipment is of central interest in the choice of design methodologies and maintenance strategies, in order to ensure safe operation of the railway network. The screwed joints in the high-speed trains are among the components which are highly subjected to fatigue. The present study aims at establishing a complete reliability-based methodology for the supervision of the equipment subjected to fatigue, by taking into account the uncertainties related to material properties, loading, manufacturing, corrosion and human errors. The results show that even with a large safety margin in fatigue design of this kind of screwed joints, lack of robustness may occur when operation conditions become uncertain. Although the high resistance to the applied load, the joint is very sensitive to friction coefficients, applied tightening and prestressing. The increase of the deterministic design margins does not improve the safety, and special care should be paid for controlling the operating and maintenance conditions.

1 INTRODUCTION

The reliability of railway equipment is of central interest in the design and maintenance, in order to ensure safe operation of the railway network of the SNCF. The screwed assemblies in the high-speed trains TGV are among the components which are highly subjected to fatigue. In addition to mechanical loading, the environmental effects (i.e. temperature, humidity, freezing…) lead to the corrosion of the thread. Moreover, during the maintenance operations, the human factor plays an important role in the assurance of the screw integrity under fatigue; hence, the reliability assessment should take account for this factor in order to estimate the screw lifetime.

The present study aims at establishing a comprehensive reliability-based methodology for the supervision of equipment subjected to fatigue, in order to optimize their maintenance on the basis of cost and reliability balance. This methodology incorporates the life cycle of the equipment, including the deterioration modes, the human errors and the uncertainties in the material properties, the geometry and the loading, as well as the impact of maintenance operations. The uncertainty analysis allows us to define the probabilistic distribution of fatigue damage as a function of train operational distance. Although the mean damage is very low, the distribution tail is largely extended to high damage levels, which strongly increase the failure probability. The corrosion in the thread induces a resisting torque during the tightening of replaced screws, and thus leads to a significant loss of the prestressing force. In order to investigate this phenomenon, the Agence d'Essai Ferroviaire of SNCF has performed several tests to measure the resisting torque as a function of corrosion levels. The human factor is taken into account by considering different scenarios during the assembly procedure. The errors in the screw type, in the tightening torque and in the cleaning of assembled surfaces have a major importance on the screw integrity. The impact of these errors is amplified by thread corrosion.

After describing the mechanical models involved in this study, the probabilistic model is given for the system parameters, including human operations. The reliability analysis is then carried out to estimate the fatigue failure probabilities in terms of operating distance for screwed assembly with and without defects and/or errors.

2 SCREWED ASSEMBLY AGING MODEL

2.1 Screwed assembly

In high-speed trains TGV, the assembly of mechanical parts is performed by the use of prestressed screws. The present study concerns the assembly connecting the vibration damping system between two coatchescoaches, as illustrated in Figure 1. During train operation, the applied force on this assembly varies in the range ±18kN. Besides the statical and dynamic loading, these assemblies are subjected to environmental conditions, such as temperature and humidity.

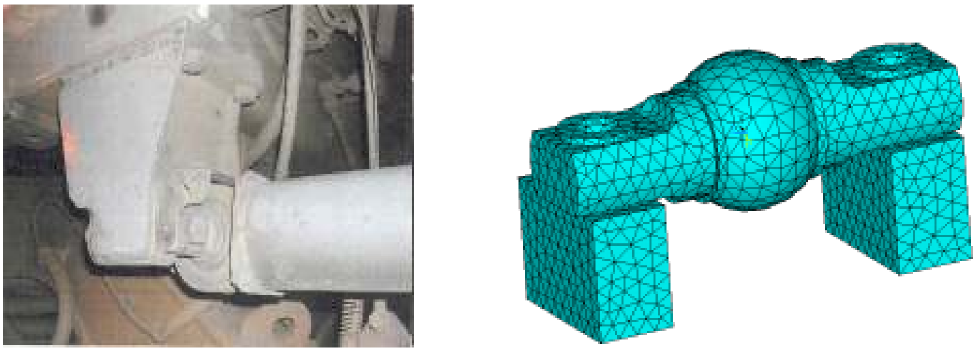

Figure 1:. Screwed assembly configuration and Finite element model.

The finite element model established by the SNCF (Figure 1) allows us to take account for real contact surface between the different components of the assembly. Due to the system configuration, the prestressing produces not only normal tension F_0 in the screw, but also bending moment M_0, which cannot be neglected. On the basis of finite element analyses, it becomes possible to calculate the normal force and the bending moment in the screw for different loading forces, varying from 0 to 80 kN. It has been observed that the alternating stress due to bending is equal to the double of the stress due to normal force, for all prestressing levels above 20 kN. At the force $F_0 = 80$ kNKN, the alternating stress is equal to 17 MPa and the total stress is 433 MPa. The ratio between the force in the screw and the applied force allows us to define the load factor for normal force λ_N and for bending moment λ_M (Figure 2). Under the prestressing force only, the load factors for normal and bending moments in the screw are interpolated by:

$$
\begin{aligned}
&\lambda_{N0} = 1000 && \text{(independant from } F_0\text{)} \\
&\lambda_{M0} = 53.782 + 0.0987\, F_0 && \text{for } F_0 > 10kN
\end{aligned}
\tag{1}
$$

where F_0 is in kN. Under the external applied load, the regression leads to the polynomial expression of these load factors as a function of the prestressing force; these factors are given by:

$$
\begin{aligned}
&\text{For } F_0 \le 50kN \ : \\
&\quad \lambda_N = -1,604\times10^{-9} F_0^5 + 5,09269\times10^{-7} F_0^4 - 6,1481\times10^{-5} F_0^3 \\
&\qquad + 3,52\times10^{-3} F_0^2 - 9,54783\times10^{-2} F_0 + 1,109785 \\
&\quad \lambda_M = 1,6812\times10^{-8} F_0^5 - 2,1834\times10^{-6} F_0^4 + 7,62715\times10^{-5} F_0^3 \\
&\qquad + 1,07414\times10^{-3} F_0^2 - 0,1125 F_0 + 2,38062 \\
&\text{For } F_0 > 50kN \ : \\
&\quad \lambda_N = 0,1268 + 10^{-4}(F_0 - 50) \\
&\quad \lambda_M = 0,5803 + \frac{6.41}{3000}(F_0 - 50)
\end{aligned}
\tag{2}
$$

Figure 2 compares the finite element and the polynomial results. The approximation is estimated to be very satisfactory for reliability analyses. These results are also conformal to the tests realized by AEF (the *Agence d'Essai Ferroviaire* of the SNCF) [1], where the force is almost zero for prestressing higher than 22kN, the load factor is 0.1 for $F_0 = 20$kN and 0.5 for $F_0 = 10$kN.

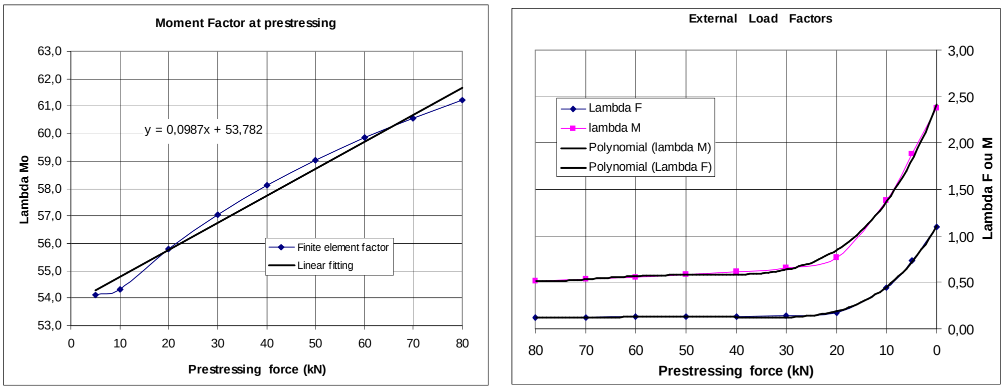

Figure 2:. Mechanical load factor in terms of prestressing.

2.2 Fatigue damage

The cumulated damage is computed on the basis of the rainflow matrices of loading, according to the measurements performed by the SNCF [2]. For each loading level $F_{e,i}$, the alternating stress σ_{a_i} is computed by:

$$\sigma_{a_i} = \frac{4\,F_{a_i}}{\pi d_0^2} + \frac{M_{a_i}\,d_0}{2\,I_0} \tag{3}$$

where the alternating normal force is given by: $F_{a_i} = \left|\lambda_N \;\Delta F_{e,i}/2\right|$ and the alternating bending moment is: $M_{a_i} = \left|\lambda_M \;\Delta F_{e,i}/2\right|$. Finally, the cumulated damage is computed by Miner's law:

$$D = \sum \frac{n_i}{2\times 10^6}\left(\frac{\sigma_{a_i}}{\sigma_D}\right)^m \tag{4}$$

where n_i is the number of cycles performed for the given load amplitude σ_{ai}, σ_D is the endurance limit, m is the fatigue constant, equal to 3 for $\sigma_{ai} < \sigma_D$ and to 5 for $\sigma_{ai} \geq \sigma_D$.

2.3 Corrosion modeling

In order to identify the corrosion effect, AEF has tested corroded screws, allowing to evaluate the resisting torque in terms of corrosion rate [3]. Black threads of diameter 18mm have been tested after an exposure to saline vapor during 92, 206 and 432 hours, followed by 4 days of drying. For an exposure less than 92h, no significant resistance has been observed. Figure 3 shows the testing machine and the measured resisting torque. The large scatter of the measured torque can be easily observed. The coefficient of variation is practically 100% and the probability distribution is almost uniform.

On the basis of saline atmospheric corrosion τ_{test}=0.1 mm/year, the fitting curve is:

$$\eta(s) = \begin{cases} 0 & for \quad s \leq 1.3 \\ 120(s-1.3) - 60(s-1.3)^{1,5} & for \quad 1.3 < s \leq 3 \\ 71 & for \quad s > 3 \end{cases} \tag{5}$$

where s is given in terms of the effective corrosion rate and the operating distance, by: $s = 3\;\tau_{Cor}\;\frac{d}{2000}$.

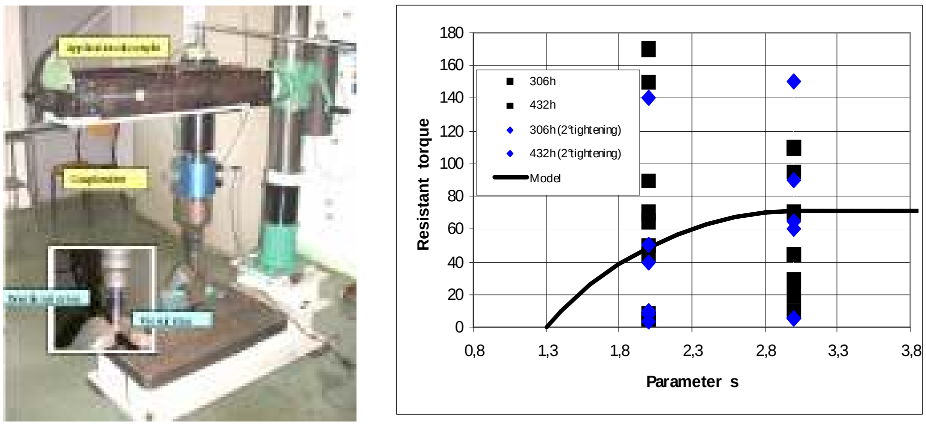

Figure 3:. Resistance torque tests and obtained results [3].

When a tightening torque C_{SER} is applied, the effective prestressing force in the screw is computed by the relationship:

$$F_0 = \frac{C_{SER} - C_{cor}}{0{,}16p + 0{,}583 d_0 \mu_f + r_m \mu_t} \tag{6}$$

where C_{cor} is the resisting corrosion torque, p is the thread step, d_0 is the nominal diameter, r_m is the mean radius of the contact area under the screw head, μ_f is the friction coefficient in the thread and μ_t is the friction coefficient under the screw head.

3 RELIABILITY ANALYSIS

3.1 Assembly defects and failure modes

The parameters influencing the screw life-cycle are as following:

- *Material characteristics*: it concerns all the material strength parameters, especially the fatigue limit, the yield strength and the parameters of the *S-N* curve.
- *Manufacturing defects*: they concern mainly the geometrical parameters, such as the parallelism of the assembled surfaces, the presence of inclusions under the screw head, the irregularity of threads, the presence of initial cracks in the thread foot and the eccentricity of drilled holes in the support.
- *Assembly errors*: they concern the mistakes in the assembly procedure, such as missing a component (screw, washers or support), the under-tightening (due to missed tightening, excessive use of the drill-tightening, bad calibration of the dynamometric tool or the presence of corrosion in the support threads), the use of wrong type of screw (longer or shorter than required or with another type of coating) and the modification of friction coefficient (due to bad cleaning of the surfaces to assemble or inclusions).

Deterioration and failure modes in service are:

- *Short-term losses*: after assembly, irreversible phenomena take place, such as relaxation and settlement of contact surfaces.
- *Extreme load*: the failure can be observed when the screw is fully yielded due to excessive loading, total separation of assembled parts, or crack propagation under permanent tension.
- *Deterioration*: this type of failure depends on the time in use where the important phenomena are: cumulated damage, tightening loss, thermal variations and corrosion; it is to note that the first two parameters depend on loading cycles and the last two parameters depend on the physical time (i.e. duration of exposure to the environment).

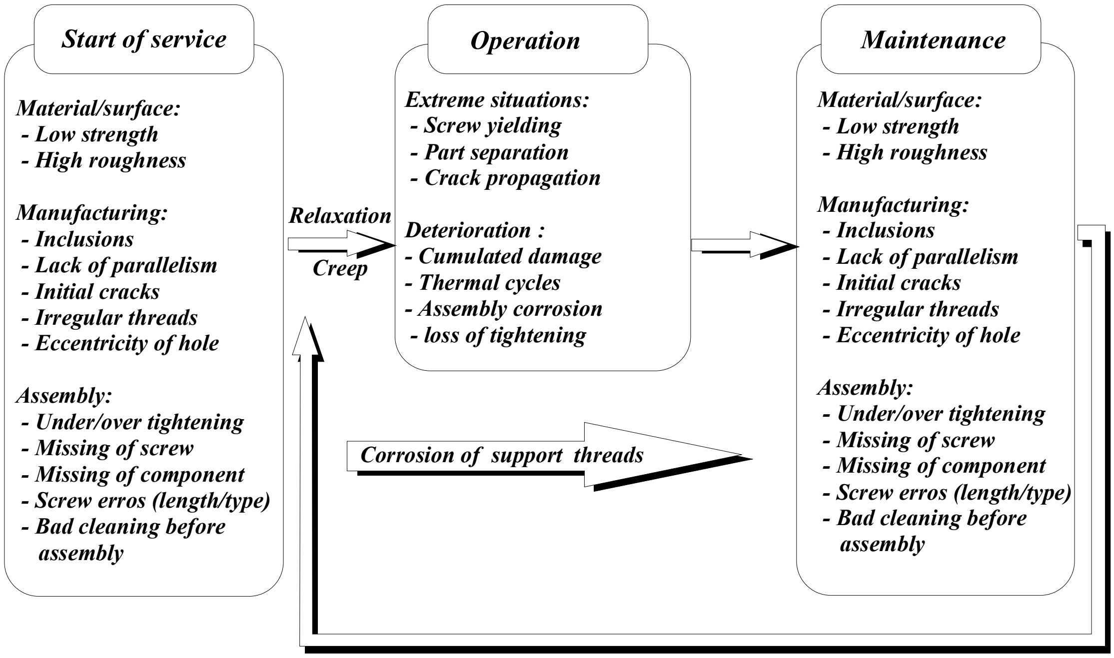

Figure 4:. Flowchart of uncertainties during the life-cyle.

The simulation of the screw system lifetime is carried out by performing Monte Carlo techniques on the system parameters and the assembly procedures in order to include all sources of uncertainties related with the assembly configuration. The human errors during assembly are introduced through the lack of tightening of the assembled parts or the use of wrong type of screw (longer or shorter than required, or with other type of coating). It also concerns the cleaning of the assembled surfaces.

Table I:. Occurrence probabilities for assembly conditions.

Event	Occurrence probability
Imperfection under screw head	10^{-3}
Insufficient thread length	10^{-3}
Hole eccentricity	10^{-3}
Over-tightening	10^{-1}
Under-tightening	10^{-4}
Wrong calibration of the tools	10^{-4}
Error in the screw type	10^{-2}
Uncleaned surfaces	10^{-1}

In addition to the assembly and human uncertainties, the system random variables are:

Table II.: Material and configuration variables.

Parameter	Mean	Standard-deviation
Endurance limit	40 MPa	4 MPa
Friction coefficient (head) μ_t	0.16	0.011
Friction coefficient (thread) μ_f	0.11	0.0066
Tightening torque	230 N.m	11.5 N.m

For the ultimate damage Δ_u, the fatigue limit state is written:

$$G_2 = \Delta_u - D \tag{7}$$

where Δ_u is usually set to unity.

3.2 Fatigue damage distribution

Monte Carlo simulations allow us to define the probability distribution of fatigue damage, as illustrated in Figure 5. Although the mean damage is very low: 0.0162 and its standard deviation is only 0.0088, it can be easlyeasily seen that the distribution tail is very extended such that high damage values still lead to significant failure probabilities. For example, the failure probability of 10^{-6} corresponds to a damage of 0.14, which is far from the mean damage by 14 times the standard deviation. It is clearly shown that the representation of damage by classical distribution models, such as lognormal and Weibull,Weibull is not appropriate to estimate the system reliability.

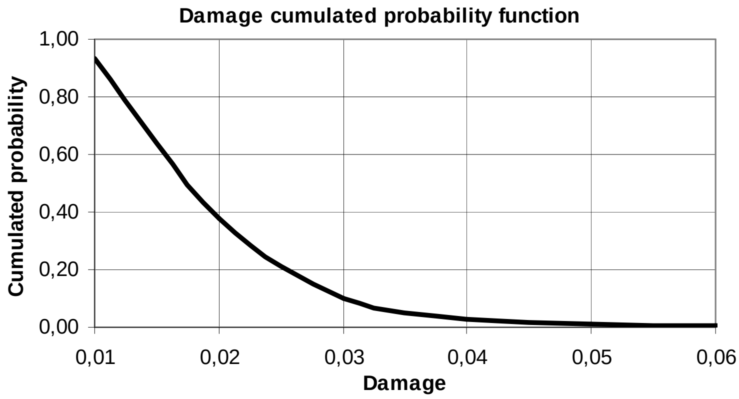

Figure 5:. Cumulated probability function for fatigue damage.

3.3 Defect influence on the failure probability

The presence of initial defect is not systematic, and therefore is subjected to an occurrence probability p_d. If an error occurs, a defect (or imperfection) is generated according to the defect distribution. For a given size of the defect d, the probability of an event with respect to the response G leads to conditional probability distribution. The probability of the response is then computed by integration over the defect variation domain, to determine the marginal distribution of the event: $G \leq 0$. However, there is a possibility that defect does not occur, while the system failure happens due to other (regular) uncertainties. Consequently, the probability of $G \leq 0$ is divided into two parts, with or without defect:

$$\Pr[G \leq 0] = \Pr\left[G \leq 0 \text{ when defect occurs} \bigcup G \leq 0 \text{ without defect}\right] \tag{8}$$

Figure 6.a shows the effect of various kinds of defects/errors on the failure probability of the screw. It underlines the important role of human activities on the system reliability, leading to loss of robustness.

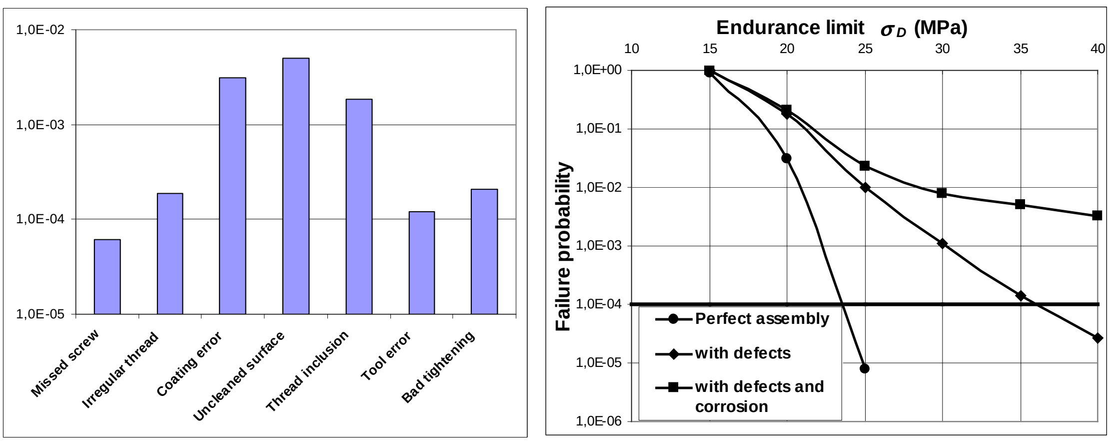

Figure 6.: Failure probability in terms of assembly defects.

For an operating distance of 4 million of kilometers (Mkkm), Figure 6.b shows the failure probability in terms of endurance limit, under different assembly configurations. When the system is perfect, the endurance limit can be reduced to 24 MPa with acceptable reliability level. When defects are considered, this limit has to be raised to 36 MPa. If these defects are combined with corrosion, no realistic endurance limit can ensure the target safety level.

3.4 Effect of effective tightening torque

Figure 7 shows the failure probability as a function of the effective torque in the screw. This probability decreases strongly for screw type errors. The decrease is also significant for defects induced by inclusions under the screw head. It is thus importance to pay attention for manufacturing and assembly conditions.

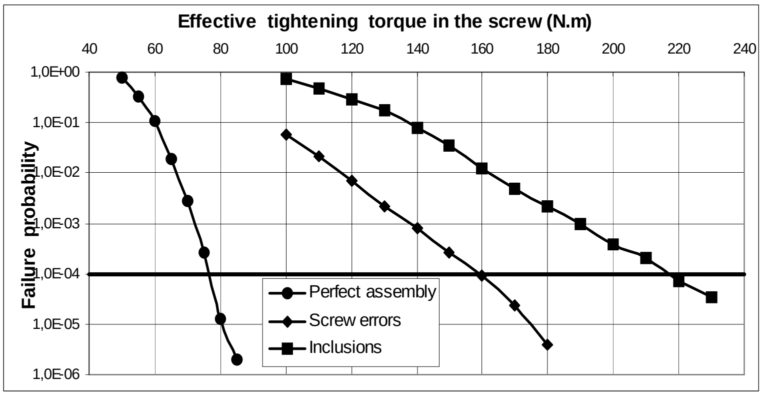

Figure 7:. Failure probability in terms of assembly defects.

3.5 Reliability assessment during life cycles

Starting from the assembly of new system, the life-cycle is composed of operating periods followed by preventive replacements of the components: shock damper, hinge, screw, lock washers and support. At the first cycle, the assembly is new and no corrosion is involved. In the following cycles, the replacement is performed for used systems and corrosion may take place. The corrosion combined with other errors or imperfections decreases the prestressing force and consequently the screw reliability. Figure 8 shows the fatigue failure probability in terms of the operating distance of the train (see also Table III). While the failure probability is naturally lower for the first cycle than for subsequent ones, the slope is higher for the new system (first cycle). It is clear that new systems present much higher safety than re-used ones; a factor of 1000 is observed for the failure probability. This safety drop is mainly due to thread corrosion combined with other types of errors, leading to significant drop in the prestressing force of the screw. Even for 4 Mkm, the failure probability for new screw remains 10 times lower than the corroded system at only 1 Mkm. It can be proposed to delay the first replacement from 1.5 Mkm (actual value) to 4 Mkm, as failure probability is still below the one for the following cycles.

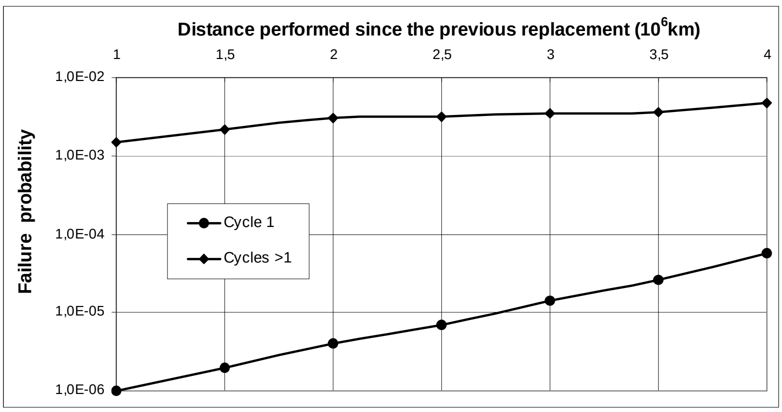

Figure 8:. Failure probability for new and used screwed assembly.

Beside the above mentioned failure probabilities, the last column in Table III indicates the effect of regular inspections (visual and torque inspection). These latter allow to avoid several kinds of errors, leading to significant decrease of the failure probability (by a factor of 10).

Table III:. Failure probabilities in terms of operating distance.

Train distance (km)	New system	Re-used system without inspection	Re-used system with inspection
1000000	1.0×10^{-6}	1.5×10^{-3}	1.5×10^{-4}
1500000	2.0×10^{-6}	2.2×10^{-3}	1.6×10^{-4}
2000000	4.0×10^{-6}	3.0×10^{-3}	1.9×10^{-4}
2500000	7.0×10^{-6}	3.2×10^{-3}	2.29×10^{-4}
3000000	2.3×10^{-5}	3.5×10^{-3}	2.30×10^{-4}
3500000	2.6×10^{-5}	3.6×10^{-3}	2.32×10^{-4}
4000000	5.8×10^{-5}	4.7×10^{-3}	2.75×10^{-4}

5. CONCLUSION

This study describes a reliability-based assessment of screwed assemblies in high-speed trains, by considering the coupling of fatigue, corrosion and human errors. It allows us to underline the significant role of corrosion in the integrity of such an assembly, due to the high resisting torque obtained when screws are placed by new ones with different length. Experimental results show that resisting torque presents a very large dispersion. Although the screw is largely over-designed from the deterministic point of view, the reliability-based analysis shows that inspections have to be included in order to significantly increase the operation intervals. Therefore, the inspection and control procedures should thus be enhanced. Beside the corrosion effect, the geometrical imperfections (thread perpendicularly, and inclusions) and human errors (use of inappropriate screw and bad cleaning of assembled surfaces) play an important role in the endurance of system reliability.

This work has also shown that even with a large safety margin in fatigue design, there is a lack of robustness when operating conditions are considered. Although the high resistance to the applied load, the assembly is still very sensitive to parameter variations: friction, tightening and prestressing. The increase of the deterministic design margins does not improve the safety, knowing the dominant influence of the human and environmental factors.

4 ACKNOWLEDGEMENTS

The authors wish to strongly acknowledge SCNF for financially supporting this research project.

5 REFERENCES

1. SNCF - Agence d'Essai Ferroviaire - "Mesure de tension de vis de fixation d'amortisseur CC Bas de la rame 365". DOC005282/S003450, 3/10/2006.
2. SNCF - "Mesure de force sur amortisseur caisse-caisse bas TGV R". SNCF 96 S2-64, MTES2 RN 97004, 1996.
3. SNCF - Agence d'Essai Ferroviaire - "Influence de l'oxydation d'un écrou sur son couple résistant". DOC005635/S003450, 27/10/2006.